Environmental Science & Technology

pubs.acs.org/est

Critical Review

The Need for Testing Isomer Profiles of Perfluoroalkyl Substances to Evaluate Treatment Processes

Kaushik Londhe, Cheng-Shiuan Lee, Carrie A. McDonough, and Arjun K. Venkatesan*

Cite This: *Environ. Sci. Technol.* 2022, 56, 15207−15219

Read Online

ACCESS | Metrics & More | Article Recommendations

ABSTRACT: Many environmentally relevant poly-/perfluoroalkyl substances (PFASs) including perfluorooctane sulfonic acid (PFOS) and perfluorooctanoic acid (PFOA) exist in different isomeric (branched and linear) forms in the natural environment. The isomeric distribution of PFASs in the environment and source waters is largely controlled by the source of contamination and varying physicochemical properties imparted by their structural differences. For example, branched isomers of PFOS are relatively more reactive and less sorptive compared to the linear analogue. As a result, the removal of branched and linear PFASs during water treatment can vary, and thus the isomeric distribution in source waters can influence the overall efficiency of the treatment process. In this paper, we highlight the need to consider the isomeric distribution of PFASs in contaminated matrices while designing appropriate remediation strategies. We additionally summarize the known occurrence and variation in the physicochemical properties of PFAS isomers influencing their detection, fate, toxicokinetics, and treatment efficiency.

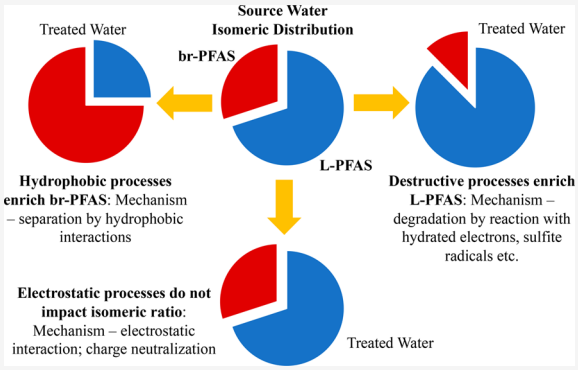

KEYWORDS: *PFAS isomers, treatment, sequestration, destructive, analytical bias*

1. INTRODUCTION

Two of the most used and studied PFASs are perfluorooctanoic acid (PFOA) and perfluorooctanesulfonic acid (PFOS). Although the intent is to manufacture linear forms of PFOA and PFOS for various applications, the type of manufacturing process used can result in the formation of different chain lengths and structural isomers of PFASs as impurities.[1−3] Electrochemical fluorination (ECF) and telomerization are the major manufacturing processes for PFOA.[1] As the ECF process is of a free-radical nature, it leads to the rearrangement and breakage of the carbon chain. This leads to the production of linear and branched isomers, mainly perfluorinated, as well as homologues of the raw material.[2] 3M Co. was the major manufacturer of PFOA from the 1950s until 2002, after which perfluorooctyl chemistries were phased out. 3M Co. produced PFOA, measured in 18 production lots over 20 years, was found to be approximately 78% linear and 22% branched.[1,2,4] Since 2002, the large scale production of linear PFOA has continued by a telomerization process and is considered to be the predominant perfluoroalkyl carboxylic acid (PFCA) manufacturing process. The telomerization process is one that involves the addition of a free radical to a starting telogen with a taxogen that is usually unsaturated. This results in chain lengthening by units of CF_2-CF_2, which when subjected to oleum oxidation can yield PFOA.[5] The result of the telomerization process is a product (e.g., PFOA) that is isomerically pure but can contain chain length impurities.

In contrast, ECF can result in greater numbers of byproducts, including branched and linear isomers that can have odd and even chain lengths.[5] PFOS has predominantly been manufactured by ECF, while telomerization sources for PFOS are unknown. 3M Co. produced PFOS from the 1950s to 2002 with a distribution of approximately 70% linear and 30% branched.[1,4] Since the phase out of PFOS by 3M Co. in 2002, production of perfluorooctane sulfonyl fluoride (POSF) and its derivatives has continued in developing countries.[1] The residual impurities, generated as byproducts of PFAS manufacturing processes, can influence the isomeric distribution of PFASs in the environment. In addition to PFOA and PFOS, other PFASs can also exhibit isomerism, including several PFCAs such as PFBA/perfluorobutanoic acid (C4), PFPeA/perfluoropentanoic acid (C5), PFHxA/perfluorohexanoic acid (C6), PFHpA/perfluoroheptanoic acid (C7), PFNA/perfluorononanoic acid (C9), PFUnA/perfluorounde-

Received: July 30, 2022
Revised: October 12, 2022
Accepted: October 16, 2022
Published: October 31, 2022

canoic acid (C11),[5,6] and perfluorosulfonic acids (PFSAs) such as PFPeS/ perfluoropentanesulfonic acid (C5), PFHxS/ perfluorohexanesulfonic acid (C6),[5,7,8] POSF,[5,9] and perfluorooctane sulfonamide (FOSA).[10]

In the past two decades, although many pieces of literature have reported multiple PFASs in diverse aquatic environments, PFAS isomers (i.e., branched or br-PFAS vs linear or L-PFAS forms) have received relatively little attention probably due to analytical difficulty and the relatively low abundance of branched isomers compared to their linear counterparts in the environment.[7,10,11] The structural difference between linear and branched PFAS isomers would determine their physical and chemical properties, such as hydrophobicity, leading to differing fates and transport mechanisms of PFAS isomers in the environment. In some instances, the concentration of branched isomers may surpass linear isomers in source waters.[7,12] This may have an impact on the overall treatment efficiency of PFASs as a few studies have highlighted the variation in the treatment efficiency between linear and branched isomers of PFASs.[13−19] For example, early breakthrough of a branched isomer from a granular activated carbon (GAC) filtration system[19,20] and preferential degradation of branched isomers over a linear form in destructive approaches[16,17,21] have been reported. In this paper, we highlight the need for differentiating the isomers of PFASs during treatment/remediation approaches as the branched-to-linear ratio in source waters can influence the overall treatment efficiency of the selected approach. The specific objectives of this critical review paper were to (i) summarize the environmental occurrence of branched and linear isomers of PFASs; (ii) highlight isomer-dependent physicochemical properties and toxicokinetics of PFASs; (iii) provide the current understanding of the variability in treatment efficacy between PFAS isomers; and (iv) highlight the impact of isomer profile on PFAS treatability.

2. ISOMERIC DISTRIBUTION OF PFASs IN THE ENVIRONMENT

Source waters can have large variations in the isomeric distribution of PFASs. One of the factors contributing to this is the proximity and type of PFAS manufacturing industry, which can greatly influence the type of PFASs released into the environment. The isomeric distribution in natural waters can also be influenced by the inherent properties of linear and branched forms. A recent study[7] summarized the global distribution of linear and branched forms of PFASs in surface water, groundwater, and seawater. They found that the ratio of br-PFAS to L-PFAS in certain surface waters was higher than expected. This was attributed to the higher normalized organic carbon to water partition coefficient[10] of L-PFAS compared to the branched forms, which is elaborated more on in the later sections. They further theorized that this could lead to stagnant water bodies such as lakes having a reduced percentage of L-PFAS than flowing bodies such as rivers, as river currents might reduce adsorption further from equilibrium conditions. Linear isomers accounted for 42−87% in lake waters and 24−89.5% in river waters, with the distribution highly dependent on the location and water source. Similar to behavior in sediments, L-PFAS sorb better to soils than the br-PFAS, leading to relatively higher concentrations of br-PFAS in groundwaters.[1,7] The br-PFAS are less retarded during subsurface transport, leading to a possible enrichment of br-PFAS in groundwater with distance.[22,23] This was also observed in a recent study conducted in El Paso County, Colorado, when the PFOS isomer concentration was analyzed at locations near and farther away from the source. The average br-PFOS contribution (br-PFOS to PFOS-total) was ∼26% near the source but increased to ∼46% at the location farthest from the source.[24] It is also important to note that biotransformation could enhance the concentration of L-PFAS in the environment due to the preferential degradation of br-PFAS.[22] However, the preferential transformation of br-PFAS precursors over L-PFAS precursors[25,26] could increase the br-PFAS/L-PFAS ratio in the environment, making concentration estimations and predictions entirely based on source tracking in environmental samples difficult.

Figure 1 summarizes the percentage of L-PFOS out of total PFOS in the environment reported in the literature. The

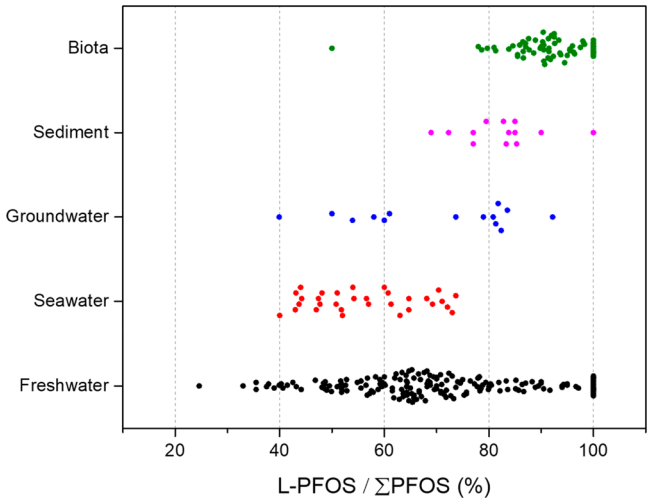

Figure 1. Representation of percentage of L-PFOS present in various environmental matrices.[1,5−7,10−12,22,23,27−51] Dots represent ratios calculated at multiple data points using either individual L-PFOS and br-PFOS values or average concentrations, depending on availability in the literature.

number of studies used to construct Figure 1 for each matrix is listed as follows: n(freshwater) = 169, n(seawater) = 31, n(groundwater) = 14, n(sediment) = 13, n(biota) = 63. The ratio (L-PFOS/∑PFOS), represented as % L-PFOS, varies significantly (p value < 0.01) between the aqueous phases, abiotic solids (sediment and suspended particles), and biota and is also influenced by different locations and studies. The largest variation of the L-PFOS was observed in freshwater systems, ranging from 25% to 100%. In contrast, % L-PFOS showed a more compact distribution in sediment and biota samples, ranging from ∼70% to 100%. These distributions seem to be impacted by the differences in the sorption properties of linear and branched isomers of PFOS. For PFOA, the L-PFOA accounted for 50% to 100% in water and 80% to 100% in sediment and biota samples.[32,33] For PFHxS, the linear L-PFHxS accounted for 64% to 99% in water and 85% to 96% in sediment and biota samples. PFOS exhibited a more considerable variation in terms of the isomeric fractionation than PFOA and PFHxS. Because of the nature of the longer chain-length of PFOS, the outcome of isomeric fractionation of L-PFOS from br-PFOS would be more distinct after a series of natural and anthropogenic processes, possibly due to the

https://doi.org/10.1021/acs.est.2c05518
Environ. Sci. Technol. 2022, 56, 15207−15219

Table 1. Reported and Predicted Physicochemical Properties of PFAS Isomers in the Literature along with Their Significance

PFAS analyte	property	reported values	difference in value for br-PFAS relative to L-PFAS (%)	significance
L-PFOS[53]	CCC bond angle (deg)	~115	~4.3−5.2 ↓	Distortion in molecular structure impacts molecule stability.
br-PFOS[53]		~109−110		
L-PFOS[53]	relative ΔG of the acidic form (normalized) (kJ/mol)	0		More positive ΔG indicates higher reactivity.
br-PFOS[53]		1.4−14.6		
L-PFOS[10]	sediment derived log K_{oc} (cm^3/g)	~3.3	~6.2−34 ↓	Higher K_{oc} values indicate higher partitioning onto sediment phase.
br-PFOS[10]		~2.2−3.1		
L-PFOA[10]		~3.1	~4.8−11 ↓	
br-PFOA[10]		~2.7−2.9		
L-PFOSA[10]		~4.4	~18 ↓	
br-PFOSA[10]		~3.6		
L-PFOSA[26]	dynamic bioconcentration factor (BCF) in carp (L/kg)	~134	~92 ↓	Higher BCF indicates longer retention in the body.
br-PFOSA[26]		10.7		
br vs L-PFOS[55]	retention in rats	NA		Branched isomers are preferentially excreted in rats compared to linear forms.
L-PFNA[56]	growth-corrected elimination rate constants in male rats	0.012−0.018	~50 ↑ (average)	Branched isomers are preferentially excreted in rats compared to linear forms.
br-PFNA[56]		0.019−0.026		
L-PFOS[54]	Human population average half-life[a] (years)	2.9	~77−81 ↓	are preferentially excreted in humans compared to linear forms
1*m*-PFOS[54]		0.55		
3/4/5*m*-PFOS[54]		0.64		
2/6*m*-PFOS[54]		0.66		
L-PFOS[57]	K_d (dissociation constant for human serum albumin)	$8(\pm4) \times 10^{-8}$	~10^5 to 5×10^5	Linear isomer preferentially binds to human serum albumin.
3*m*-PFOS		$4(\pm2) \times 10^{-4}$		
4*m*-PFOS		$8(\pm1) \times 10^{-5}$		
5*m*-PFOS		$9(\pm5) \times 10^{-5}$		
L-PFOA		$1(\pm9) \times 10^{-4}$	~200−300	
3*m*-PFOA		$4(\pm2) \times 10^{-4}$		
4*m*-PFOA		$3(\pm2) \times 10^{-4}$		
L-PFOS[58]	drinking water equivalent levels (DWELs) in $\mu g/L$[53]	0.29	206−638 ↑	Higher DWEL levels suggest less effectiveness in reducing thyroid hormonal blood levels.
1*m*-PFOS[58]		1.26		
2*m*-PFOS [58]		1.84		
3*m*-PFOS[58]		1.40		
4*m*-PFOS[58]		1.75		
5*m*-PFOS[58]		2.14		
6*m*-PFOS[58]		0.89		
br-PFPeA[8]	predicted octanol−water partitioning coefficient, dry (log $K_{OW,\ dry}$)	3.24−3.42	0.3−5.5 ↓	Higher K_{OW} values indicate higher potential for bioaccumulation.
L-PFPeA[8]		3.43		
br-PFHxA[8]		3.54−4.01	1.2−13 ↓	
L-PFHxA[8]		4.06		
br-PFHpA[8]		3.61−4.64	0.6−23 ↓	
L-PFHpA[8]		4.67		

[a]Model considers original serum levels in humans. ↑ and ↓ indicate increase and decrease respectively in the percentage value of the property being considered. Note: *m*-PFAS indicates the branching at the *m*th carbon.

greater variation in physicochemical properties reported between the isomeric forms with increasing chain length.[8]

Several factors are known to govern the composition of PFAS isomers in water. Some of these factors include (i) the initial isomeric distribution from manufacturing process release; (ii) interactions with and effects of both natural and biological processes; and (iii) isomer-specific precursor transformations. First of all, the release from manufacturing processes (e.g., ECF and telomerization processes) can directly determine the isomeric distribution of PFASs in water. Natural and anthropogenic processes can further modify the ratio between linear and branched isomers. For natural processes in water, L-PFAS would preferentially sorb to suspended particles, sediments, and phytoplankton cells, therefore leading to scavenging of L-PFAS from the aqueous phase and the enrichment of L-PFAS in abiotic solids[10] and algal cells. Floating foam formed by natural organic matter could also take up more L-PFAS than br-PFAS, leaving more br-PFAS in the bulk of water. Preferential degradation of branched over the linear precursors can increase the concentration of br-PFAS in

https://doi.org/10.1021/acs.est.2c05518
Environ. Sci. Technol. 2022, 56, 15207−15219

the environment. The distribution among the branched isomer products can also differ due to the difference in biotransformation rates of br-PFAS precursors.[26] In organisms, L-PFAS is known to be more bioaccumulative and br-PFAS can be eliminated faster, explaining why L-PFASs are often highly enriched in biota (Figure 1).

3. VARIATION IN PHYSICOCHEMICAL PROPERTIES OF DIFFERENT PFAS ISOMERS

There are only a few studies that report the variation in physicochemical properties of PFAS isomers as summarized in Table 1.[8,9,52−54] In a study done by Chen et al. (2015), the field-based water sediment distribution coefficients (K_d) were used to calculate the organic carbon−water partitioning coefficient (K_{OC}) values.[10] For PFOA, the L-PFOA had a log K_{oc} value of 3.11 ± 0.38 cm^3/g, whereas the iso, 4m, and 5m (br-PFOA) forms had relatively lower log K_{oc} values of 2.96 ± 0.48, 2.77 ± 0.53, and 2.82 ± 0.51 cm^3/g, respectively.

A similar trend was observed for PFOS where the L-PFOS had the highest log K_{oc} value of 3.38 ± 0.43 cm^3/g, and the values for br-PFOS ranged from 2.65−3.17 cm^3/g.[10] These values suggest that the L-PFASs are more likely to be preferentially distributed (∼16% more) in the particulate phase than the br-PFASs. This could explain the lower-than-expected concentrations of the L-PFOS in surface and groundwaters (as shown in Figure 1) as the preferential adsorption would enrich the br-PFOS/L-PFOS ratios in the aqueous phase.

Unlike traditional lipophilic persistent organic pollutants that partition primarily to storage lipids, PFAS bioaccumulation factors and tissue distribution appear to be influenced both by interactions with transporter proteins as well as partitioning to phospholipids.[59,60] The composition of branched and linear PFOS in human serum and their association with adverse health outcomes were recently reviewed.[7] Branched PFOS isomers tend to have shorter half-lives in the human body than linear PFOS, likely due to the variation in affinity for lipids and transporter proteins, including varying binding affinities for human serum albumin and organic anion transport proteins.[54,61,62] The average half-lives for L-PFOS were found to be 4.4−5.3 times greater than that of br-PFOS in a cohort with AFFF-impacted drinking water.[54] It is important to note that the serum levels were obtained after subtracting general population levels or were replaced with half of the these levels, if the serum PFAS levels, post subtraction, were less than half of the background levels.[54] This may have implications for remediation targets and safe drinking water levels that are defined for branched versus linear isomers. Differences in toxicokinetics have been considered when developing drinking water equivalent levels (DWELs), resulting in lower values for L-PFOS (0.26 μg/L) versus br-PFOS isomers (0.89−2.14 μg/L), in this case suggesting that the linear isomers pose a greater risk for lowering thyroid hormonal blood levels.[58] For the most part, current regulatory levels do not differentiate between branched and linear isomers. In cases where branched isomers make up a significant portion of total drinking water contamination, this may mean that recommended levels would become more conservative. While branched isomers generally display more rapid elimination rates and lower bioaccumulation factors, it is important to note that each branched isomer is distinct. In some studies, certain branched isomers have displayed longer elimination rates than L-PFOS.[56] Due to branched isomers being summed during analysis, there is very little information on specific isomers, and elimination rates reported for the human population usually represent an average for multiple isomers with unknown composition. At this time, there are not sufficient data related to differences in relative source contributions and reference doses for branched versus linear isomers to safely define distinct isomer-specific drinking water guidelines.

Despite their faster elimination rates, summed branched PFOS is detected at concentrations similar to linear isomers in serum from some populations, with typical % br-PFOS ranging from 30 to 50%.[7] In contrast, most wildlife studies report lower contributions from branched isomers (Figure 1). This may indicate greater direct exposure of humans to PFAS precursors, which are transformed *in vivo* to form perfluoroalkyl acids (PFAAs), with preferential formation of branched isomers.[26,63] This elevated exposure likely arises from sources other than drinking water, such as certain foods, paper products, textiles, and other consumer products.[64−66]

The structural and thermodynamic properties of the PFAS isomers can provide insights into their overall stability and susceptibility to degradation. It was found that all the carbon−carbon−carbon (CCC) angles for L-PFOA were approximately 115°, whereas in br-PFOS, the CCC angles where the -CF_3 group was bonded were approximately 109−110°.[53] This distortion in the CCC angle in the backbone structure can affect the stability of the br-PFAS,[53] making them less stable and more susceptible to degradation. This can be further elucidated by comparing the Gibbs free energy (ΔG) of the PFOS isomers by setting the least positive value to zero for relative comparison. It was observed that, for the acidic forms, L-PFOS had the least positive value of ΔG and was set to zero, while 1-CF_3-PFOS, 2-CF_3-PFOS, 3-CF_3-PFOS, 4-CF_3-PFOS, 5-CF_3-PFOS, and 6-CF_3-PFOS had ΔG values ranging from 1.4−14.6 kJ/mol, where *n*-CF_3-PFOS indicates branching at the carbon position '*n*'.[53] A more positive ΔG value for br-PFAS indicates that these isomers are more likely to be reactive and degraded by reactions with species such as hydrated electrons or hydroxyl radicals[53] than their linear counterparts. However, it is important to note that the study done by Rayne et al. (2010) using different models to predict the ΔG values of isomers of PFOS and PFOA pointed out the lack of utility of using thermodynamic data for PFAS isomeric distribution studies. When the authors studied the thermodynamic stability of isomeric forms of alkanes such as hexane and heptane, the modeling data agreed with the experimental data in stating that the linear form of alkanes was the least stable thermodynamically. The model predicted similar results for PFASs, where the L-PFOS and L-PFOA were predicted to be the least stable, with the stability increasing with branching. The authors attributed this to a lack of thermodynamic data available for PFCAs and stated that improved models might be essential for accurate data sets,[9] which could bridge the gap between predicted and experimental data, where L-PFAS have been found to be the dominant isomers. As a result, although certain models may predict L-PFAS as the most stable form under certain conditions, more information is needed to accurately predict stability of various PFAS isomers from mere thermodynamic data.

A similar conclusion, favoring the stability of the L-PFASs, however, can also be drawn based on the bond dissociation energies (BDE) of L-PFAS and br-PFAS. Previous studies have reported that the BDE values were ranked in the order of

https://doi.org/10.1021/acs.est.2c05518
Environ. Sci. Technol. 2022, 56, 15207−15219

Table 2. Summary of Analytical Techniques Used for Differentiating Branched and Linear Isomers

column	column dimensions	analytical reagents	injection volume	instrument	PFAS isomers (with count) studied[a]	study
FluoroSep-RP Octyl column	150 × 2.1 mm, 3 μm particle size	methanol and water (3 mM formic acid in water, adjusted to pH 4.0 with ammonia)	10 μL	LC-MS/MS	PFOA (4), PFOS (6), PFOSA (2)	Chen et al. 2015[10]
FluoroSep RP Octyl column	150 × 2.1 mm, 3 μm particle size	methanol and water (adjusted to pH 4.0 with ammonium formate)	20 μL	HPLC−MS/MS	N-EtFOSA(12), FOSA (6), PFHpA (4), PFHxA (8), PFOA (10), PFOS (11), PFNA (11), PFDA (3), PFUnA (7), PFDoA (18)	Benskin et al. 2007[76]
BEH C18 column	2.1 × 50 mm, 1.7 μm particle size	methanol and 2 mM ammonium acetate	1 μL	UPLC MS-MS	PFOS (2)	Gu et al. 2016[16]
Hypersil Gold precolumn + Betasil C18 column	10 × 2.1 mm, 5 μm particle size + 50 × 2.1 mm, 5 μm particle size respectively	methanol and water (both with 10 mM aqueous ammonium acetate	10 μL	HPLC	PFHxS (2), PFOS (2)	Belkouteb et al. 2020,[13] Ahrens et al. 2016[77]
Zorbax Extend-C18 column	2.1 × 50 mm, 1.8 μm particle size	methanol and ammonium acetate in water (pH 6)	10 μL	HPLC + Q-TOF	PFOS (8)	Trojanowicz et al. 2019[78]
Zorbax RRHD Eclipse Plus C18 column	100 mm × 2.1 mm, 1.8 μm particle size	methanol and 5 mM ammonium acetate in water		LC-MS/MS	PFOS (2)	Park et al. 2020[19]
Zorbax Eclipse Plus C18 column	4.6 mm × 100 mm, 3.5 μm particle size	3% methanol in water and 10 mM ammonium acetate in methanol		HPLC + MS/MS	PFPeA, PFHxA, PFHpA, PFOA, PFNA, PFBS, PFPeS, PFHxS, PFHpS PFOS, FPeSA, FHxSA, FOSA, N-TAmP, FHxSA (2 for each)	Rodowa et al. 2020,[20] Barzen-Hanson et al. 2017[79]
C18, analytical column	100 × 3.0 mm, 5 μm particle size	methanol and 20 mM ammonium acetate in water	1 mL	QTOF	PFOS, PFHpS, PFHxS, PFOA, and PFHpA (2 for each)	Tenorio et al. 2020[70]
Perfluorinated phenyl (PFP) phase + X-Terra C18 phase	150 × 2.1 mm, 5 μm particle size 100 Å pore size + 100 × 3.0 mm, 3.5 μm particle size, 125 Å pore size respectively	methanol and 4 mM ammonium acetate in water		ion trap mass spectrometer (LCQ	PFOS (7)	Langlois et al. 2006[80]
Thermo Acclaim 120 C18 column + FluoroSep RP Octyl column (3 mm, 2.1 mm150 mm	4.6 × 150 mm, 5 μm particle size + 2.1 × 150 mm, 3 μm particle size	acetonitrile and 10 mM ammonium acetate in water		HPLC + MS/MS	PFHxS (2), PFOS (6), PFOA (6)	Gao et al. 2019[23]

[a]Note: 2 indicates br (grouped together/single isomer studied) and L-PFAS.

https://doi.org/10.1021/acs.est.2c05518
Environ. Sci. Technol. 2022, 56, 15207−15219

tertiary < secondary < primary bonds.[67] This means that the initial C−F bond cleavage occurs at the bond with the lowest BDE, i.e., the tertiary C−C bond.[67] Thus, it can be expected for br-PFASs to behave differently during various physical and chemical treatment processes impacting the overall PFAS treatment efficiency.

4. IMPACT OF ISOMERIC PROPERTIES ON TREATMENT PERFORMANCE

Difference in the physicochemical properties between PFAS isomers and their relative levels in source waters can influence the overall treatment efficiency of PFAS. In the case of adsorption techniques such as GAC filtration, where the dominant mechanism is hydrophobic interaction with contaminants, the L-PFASs tend to show better removal than the br-PFASs. This has been reported in previous studies[13−15,19] using GACs as well as materials such as Geothite.[68] A study involving a pilot scale GAC system indicated that the br-PFAS showed an earlier breakthrough than their respective linear isomer, attributed to better interactions between L-PFAS and GAC.[20] In another study involving two-stage carbon filters, the relative percentage of br-PFOS kept increasing in treated waters as water passed through the filters.[14] This would also imply that the br-PFAS would exhibit an earlier breakthrough from GAC columns than L-PFAS.

In the case of adsorption processes involving charged interactions as the dominant mechanism, there would be minimal effect on the final L-PFAS/br-PFAS ratio after treatment.[15,18] In a previous study that utilized anion exchange resins (AIX) and GAC to remove PFCAs, PFSAs, and FOSA, similar removals were observed for PFOS, PFHxS, and FOSA isomers using AIX, but branched isomers showed lower removals using GAC.[15] In another study to remove PFCAs and PFSAs utilizing magnetic AIX, identical uptake was observed for br-PFAS and L-PFAS.[18] As br-PFAS and L-PFAS will have similar electrostatic interactions, we hypothesize that treatment techniques that rely on charged interactions with PFAS will not have an observable impact on the isomeric distribution of PFASs in treated water.

ΔG and the BDE will play a crucial role when considering the interactions of PFAS isomers with reactive species during chemical treatment processes. As mentioned previously, in certain cases, the br-PFAS possesses more positive ΔG (thus more reactive) and a lower BDE than L-PFAS. This makes them more prone to an attack by reducing species and susceptibility to degradation. In a study done to evaluate reductive defluorination of PFOS, br-PFOS showed more susceptibility to reductive dehalogenation than L-PFOS.[21] When PFOS degradation was performed by electron beam, br-PFOS preferentially degraded over L-PFOS and this was attributed to higher electron affinity of branched isomers.[17] Similar results were observed for PFOS using a UV-sulfite system and using photodegradation[69] where the br-PFOS degraded faster than L-PFOS due to the tertiary $-CF_3$ group being more susceptible to degradation.[16] In another study done by using UV-sulfite to degrade PFASs of different chain lengths and functional groups, rate constants for degradation for branched forms (>2 h^{-1}) of PFOS, PFHpA, PFHpS, PFHxS, and PFOA were an order of magnitude higher than the corresponding linear forms (0.018−0.440 h^{-1}).[70] Thus, it can be concurred that contrary to adsorption techniques, destructive treatment will enrich the L-PFAS-to-br-PFAS ratio due to the preferential degradation of branched isomers. However, this may not be valid in certain destructive techniques such as electrochemical oxidation processes (eAOPs) that employ a two-step mechanism. This technique consists of inactive electrodes such as boron-doped diamond or Magneli-phase titanium suboxide anodes, where the first step is the adsorption of PFAS on the surface of the electrodes, followed by a direct electron transfer[68,71−74] (DET) reaction and mineralization of the PFAS radical by hydroxyl radicals. As the first step of this technique involves a sorption step, the linear isomers would be preferentially adsorbed and partake in the DET and get degraded in the process. This may lead to a scenario where more L-PFAS are degraded than br-PFAS, leading to a possible enrichment in the br-PFAS in the treated water. Thus, as more and more destructive techniques involving multistep mechanisms are looked at for PFAS treatment, it is essential to understand the behavior and monitor the final concentrations of PFAS isomers.

5. ANALYTICAL CHALLENGES IN QUANTIFYING ISOMERS OF PFAS

EPA Methods 537.1 and 533 are commonly used by research and commercial laboratories for PFAS measurements in water matrices. However, the fraction of linear and branched isomers for the same compound can vary based on the supplier for the analytical standards. This was clearly shown by Vyas et al. (2007) that for potassium perfluorooctane sulfonate (K-PFOS) from different manufacturers the percentage of linear form varied from 76.0 ± 1.9% to 82.2 ± 0.9%.[75] Similarly, for perfluorooctane sulfonyl fluoride, the linear form accounted for 71.8 ± 1.3% to 74 ± 1.6%, based on the manufacturer.[75] In the majority of commercially available PFAS standards and neat materials, the relative mass or concentration of linear and branched PFAS is often not reported. ^{19}F NMR is required to accurately determine the fraction of the isomeric composition. Although liquid chromatography tandem mass spectrometer (LC-MS/MS) can differentiate branched and linear PFASs (for PFOS, PFHxS, etc.), the EPA methods require the users to integrate both peaks together and report total concentration rather than isomeric-specific concentrations. Ideally, the assumption is that the peak area can reflect the mass of the uncharacterized isomers in samples. However, the instrument sensitivity, the collision energy, and the abundant ion transitions of each isomer is different and therefore can potentially lead to a bias in quantification of total PFAS levels. A summary of analytical techniques including column specifications, reagents utilized, etc. to identify different PFAS isomers by previous studies can be found in Table 2.

Previous researchers have also observed in the case of PFOS that if the isomer profile in the sample and the quantification standards were not identical, this could lead to an analytical bias of unknown proportion.[5,81] This was further quantified by a later study that used individual, purified PFAS isomers to compare the response factors, albeit relative to the linear isomer. The 1-CF_3 PFOS was monitored using a mass to charge (m/z) ratio of 80, whereas 4,4-CF_3 $m2$- and 4,5CF_3-PFOS (br-PFOS) were monitored using a ratio of 99. It was observed that at least one PFOS isomer was missing from the final chromatogram, irrespective of the product ion used.[1,82] This could lead to underreporting of certain isomers, leading to an analytical bias being introduced during quantification. An example chromatogram featuring br-PFAS and L-PFAS with different precursor−product pairs is shown in Figure 2. It is

https://doi.org/10.1021/acs.est.2c05518
Environ. Sci. Technol. 2022, 56, 15207−15219

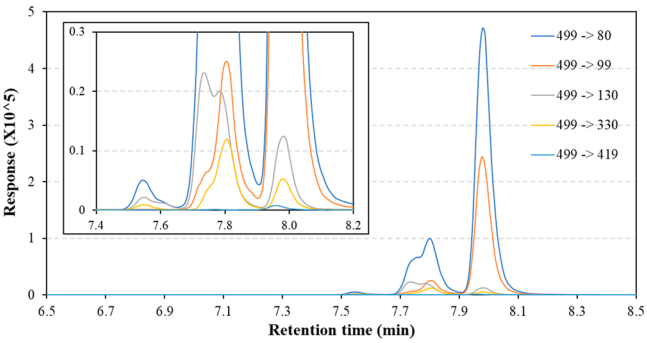

Figure 2. LC-MS/MS chromatogram representing linear and branched forms of PFOS isomers. The response is from 5 pg injection. Figure inset is a zoomed in version of the chromatogram with retention times of 7.4 to 8.2 min featuring peaks resulting from different m/z transitions.

challenging to separate and quantify every single branched isomer, and therefore it is understandable that EPA Methods 537.1 and 533 only require determining linear and "bulk" branched isomers. Transitions 499 → 80 and 499 → 99 are chosen for PFOS quantification and qualification because m/z 80 and m/z 90 are the most common products among all PFOS isomers, and m/z 80 gives great sensitivity. A systematic bias could also be introduced during analysis if the concentration of branched isomers in samples reaches the detection limit. This could lead to the contribution of the linear form for PFAS to be incorrectly reported as 100%. This bias can be eliminated by reporting the ratio of each individually detected branched isomer to the linear isomer.[1]

To demonstrate the uncertainty that can occur with different calibration methods, as an example here we use the K-PFOS standard purchased from Wellington Lab Inc. with % L-PFOS of 78.8%. Calibration Method 1 involved the addition of peak areas of linear and branched isomers, creating one calibration curve to calculate the total PFOS concentration and then calculating linear and branched PFOS concentrations separately based on the fraction of the peak area. Calibration method 2 involved the generation of two calibration curves based on the peak areas for linear and branched PFOS individually with the well-characterized standard, calculating their concentrations separately and then summing the values to determine the total PFOS concentration. Both linear and quadratic regressions were used for creating calibration curves (Figure 3). To simulate the uncertainty in these two methods, we fixed the total peak area equivalent to 1 μg-total PFOS/L but varied the percentage of the linear isomer's peak from 0% to 100% to calculate total PFOS concentrations using Methods 1 and 2. The simulated result is shown in Figure 3. Because the total peak area (linear plus branched) is fixed, the calculated total PFOS concentrations by Method 1 were the same

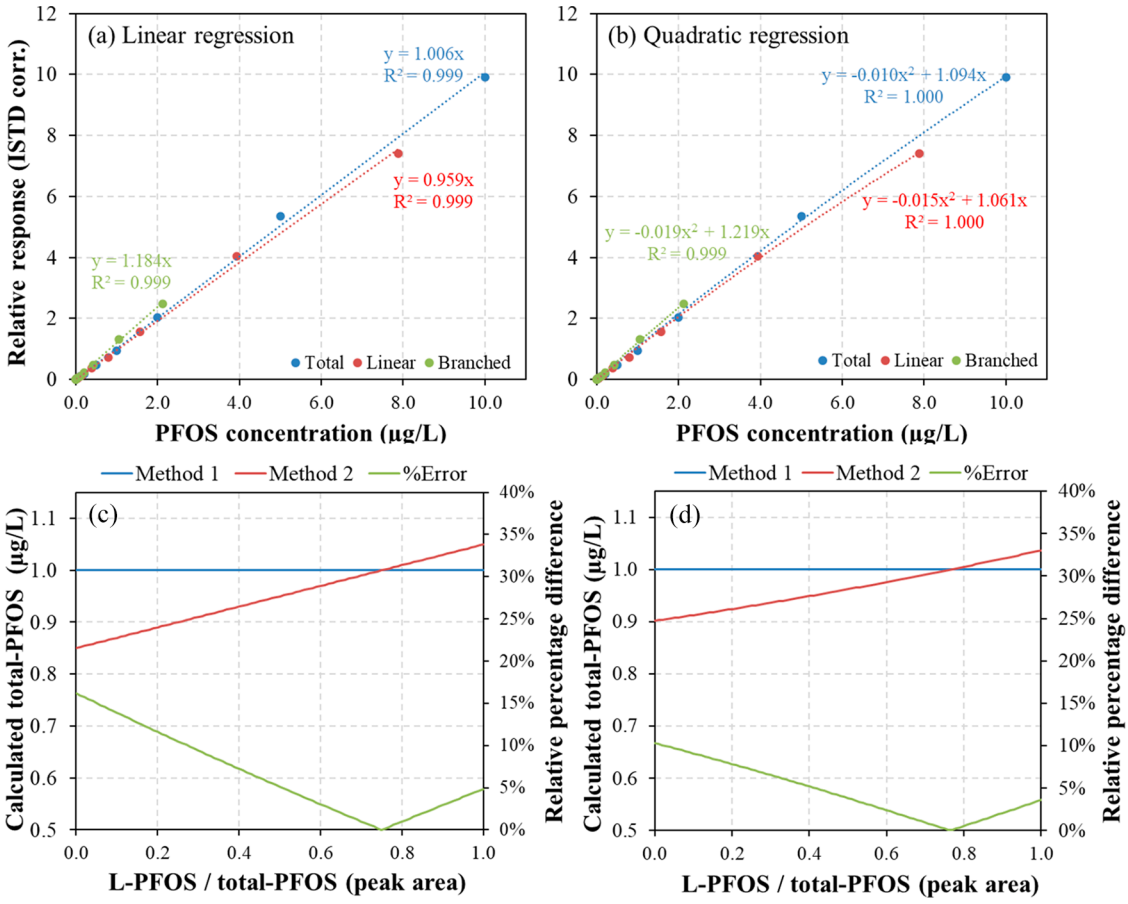

Figure 3. Calibration curves of K-PFOS using (a) linear and (b) quadratic regressions. The calibration ranges from 0.010 to 10.0 μg/L. The intercept is forced to zero. Simulation of the calculated total PFOS concentration using Methods 1 and 2 with (c) linear regression and (d) quadratic regression, as a function of the peak area of L-PFOS/total-PFOS. Green lines represent the relative percentage difference (RPD) between two values calculated by Methods 1 and 2, respectively.

https://doi.org/10.1021/acs.est.2c05518
Environ. Sci. Technol. 2022, 56, 15207−15219

Table 3. Summarizing Removal Mechanism, Advantages and Disadvantages of Treatment Techniques for Removal of PFAS Isomers[a]

technology	type of treatment	removal/breakdown mechanism	PFAS studies	difference in removal for br-PFAS relative to L-PFAS	removal summary	advantages	disadvantages
GAC filtration[13−15,19,20]	sequestration	adsorption-hydrophobicity dependent	5 PFSAs, 13 PFCAs, 2 FOSAs, 2 FOSAAs, 2 FOSEs, 1 FTSA	8−29% ↓	br-PFAS showed earlier breakthrough/poor removal vs L-PFAS	cost-effective and good removal of hydrophobic L-PFAS	relatively poor removal/early breakthrough of br-PFAS, PFAS-concentrated waste stream
AIX[18]		adsorption-electrostatic interactions	6 PFCAs, 2 PFSAs		similar removal for br and L-PFAS	Isomerism did not impact removal efficiency.	fouling issues, high initial costs, PFAS-concentrated waste stream
AIX[15]			10 PFCAs, 3 PFSAs, 1 FOSA	0−5% ↓	L-PFOS showed better removal	preferential removal of L-PFAS	
electrocoagulation[87]		Floc formation followed by sorption	5 PFCAs, 1 PFSA				relatively poor removal of br-PFAS, PFAS concentrated waste stream
eAOP[74,88,89]	destructive	oxidation by OH·	7 PFCAs, 3 PFSAs		similar removal for br and L-PFAS	Isomerism did not impact removal efficiency.	high initial costs (e.g., electrode materials)
E-beam/gamma irradiation[17,90−92]		reactions with oxidative/reductive species	1 PFSA, 1 PFCA, 1 FTS	∼78% ↑ (degradation)	br-PFAS preferentially degraded	can actually breakdown C−F bonds in br and L-PFAS	breaking down L-PFAS requires more energy.
				17−30% ↑ (rate constant)	L-PFAS showed more resistance to degradation		high energy requirements, capital costs
advanced reduction processes[16,21,70,93]		reactions with reductive species	7 PFSAs, 5 PFCAs, 3 FTS	20−87% ↑			
photocatalyis[94,95]			PFOS	rate constants were 4−965× ↑			
photodegradation[69]		direct reactions with UV irradiation	PFOS	7−170% ↑ (rate constants)			

[a]Note: Table created using previous studies that have compared the removal/degradation efficiencies of br and L-PFAS.

https://doi.org/10.1021/acs.est.2c05518
Environ. Sci. Technol. 2022, 56, 15207−15219

regardless of the fraction of L-PFOS (Figure 3c,d, blue lines). In contrast, the calculated total PFOS concentrations by Method 2 (Figure 3c,d, red lines) showed a clear deviation from Method 1. Two methods have a similar result only if the fraction of L-PFOS in the sample is very close to the calibration standard (where the blue and red lines cross, L-PFOS/total-PFOS = ~0.75). The deviation becomes greater as the L-PFOS fraction declines or increases. The relative percentage deviation (Figure 3c,d, green lines) between two methods can be up to 15% in certain cases, and the deviation is primarily contributed by branched isomers. It should be noted that such deviation can vary a lot from one analytical batch to another, depending on the quality of the calibration curves established. This simulation demonstrates that biases could occur merely due to the selection of calibration methods and PFAS standards. As a result, the concentrations of L-PFAS and br-PFAS reported in the literature and summarized in Figure 1 can differ based on the method employed. Thus, for accurate quantitation of PFAS isomers in samples, it is important to select not only the correct analytical techniques mentioned in Table 2 but also the PFAS standards and the methods that can distinguish different PFAS isomers.

6. THE NEED FOR TESTING PFAS ISOMERS IN SOURCE WATERS AND TREATMENT PROCESSES

The scientific community has not recognized the need to differentiate PFAS isomers during development and testing of treatment technologies. This is partly due to the absence of any differentiation in the regulation of PFAS isomers and limitations with available analytical methods as highlighted above. Many U.S. states have proposed stringent drinking water limits for selected PFASs in drinking water at concentrations lower than 10 ng/L.[83−86] Changes in the isomeric profile in source water can lead to preferential treatment of L- or br-PFAS and depending on the type of technologies used, and some scenarios may lead to concentrations exceeding the regulatory limit in treated water. Although the differences in properties and the resulting fate of different PFAS isomers during treatment may seem to be small, at such low regulatory limits, these differences could influence the overall treatment efficiency. For example, the presence of higher levels of br-PFAS in source waters can impact GAC performance by reducing the life of the carbon requiring frequent changeouts and thus increasing the cost of treatment. For many destructive approaches, like advanced oxidation processes (AOPs), the treatment conditions are optimized in laboratory settings prior to full-scale operation. If the PFAS isomer profile in the source water utilized for the optimization process is different from actual field conditions, the treatment technology may not perform ideally to achieve treatment goals.

This can be elucidated by Figure 4 that simulates the PFOS (total) concentration after treatment utilizing destructive techniques (Figure 4a) and sequestration techniques (Figure 4b) as a function of L-PFOS in source water. The model considers initial concentrations of PFOS in source water to range from 50 to 100 ppt. The extreme scenarios are defined by the treatment of PFOS from 100 ppt with the lowest degradation efficiency reported in the literature (black curve) and by the treatment of PFOS from 50 ppt with the highest degradation efficiency reported in the literature for br-PFOS and L-PFOS (red curve). The upper and lower limits of the curve are chosen based on analysis of EPA's UCMR3 data that

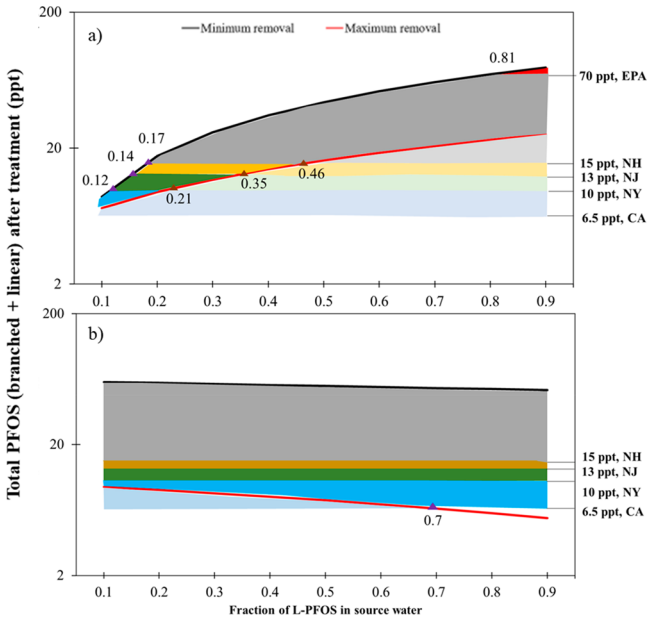

Figure 4. Simulation of total PFOS after treatment using (a) destructive techniques and (b) sequestration techniques as a function of fraction of L-PFOS in the source water. The upper black curve represents a scenario featuring minimum removal percent efficiencies for L-PFOS and br-PFOS at (a) 13 and 90%[16] and (b) 35 and 25%,[98] respectively, when treating a source water with an initial total PFOS concentration of 100 ppt. The bottom red curve represents a scenario featuring maximum removal percent efficiencies for L-PFOS and br-PFOS at (a) 45 and 100%[17] and (b) 90 and 80%,[15] respectively, when treating a source water with an initial total PFOS concentration of 50 ppt. The shaded regions below the curve represent scenarios showing violation of individual state and federal PFOS limits after treatment. Numbers adjacent to the curves indicate the fraction of L-PFOS at which a particular violation occur.

reported a mean PFOS concentration of 77 ppt in source water.[96] For destructive techniques, the model considers efficiencies of 100% (br-PFOS) and 45% (L-PFOS) reported for the UV-sulfite technique[16] to generate the line of highest degradation and of 90% (br-PFOS) and 13% (L-PFOS) reported using the e-beam technique as the line of lowest degradation.[17] Similarly, the model considers removal efficiencies of 90% (L-PFOS) and 80% (br-PFOS) using GACs[15] and 35% (L-PFOS) and 25% (br-PFOS) estimated for treatment using coagulation[97,98] as lines of highest and lowest removal, respectively. The shaded regions below the corresponding curve represent violation of state regulations or federal limits as a function of the L-PFOS fraction.

For destructive techniques (Figure 4a), it can be noted that the total PFOS concentration post-treatment increases with the increase in % L-PFOS. This can result in a violation of California reporting limit (6.5 ppt, notification limit) first and eventually the New York State limit (10 ppt) at a L-PFOS fraction of 0.21 for the high degradation scenario. As the fraction of L-PFOS increases, the final PFOS concentration (total) can violate the New Jersey State limit (13 ppt) and New Hampshire State limit (15 ppt) at L-PFOS fractions of 0.35 and 0.46, respectively. A similar trend occurs for the line with lowest removal observed in Figure 4a; however, the individual U.S. state violations occur at a much lower fraction of L-PFOS in the water, shown by numbers adjacent to the fraction of L-PFOS at which the violation occurs, eventually

https://doi.org/10.1021/acs.est.2c05518
Environ. Sci. Technol. 2022, 56, 15207−15219

violating the EPA drinking water limit (70 ppt) at an L-PFOS fraction of 0.81. For sequestration techniques, California State regulation is violated using a coagulation approach to treat 50 ppt initial concentration of PFAS (Figure 4a), but as the fraction L-PFOS increases, the system performance improves below the California State limit at a fraction of ∼0.7. It is important to note that this model does not include the interim updated health advisory limit of 20 parts per quadrillion or 0.02 ppt published by the EPA.[99] However, even at the lowest initial PFOS concentrations used in the model of 50 ppt and at highest removal efficiencies of 90 and 80% for L-PFOS and br-PFOS, respectively, the lowest value attained of total PFOS is still ∼5.5 ppt, approximately 275 times higher than the interim health advisory limit proposed for PFOS of 0.02 ppt.[99]

This simulation demonstrates that the same treatment system can violate or abide by a regulation limit if the isomeric composition of the source water changes over time. This simulation highlights the need for considering the isomeric distribution of PFAS in source waters and during the design/selection of treatment approaches for PFAS. This critical review highlights the need to consider the following when studying PFASs that exhibit isomers:

(i) Standardized analytical methods are needed to differentiate and quantify the isomeric forms of PFASs in the source waters.
(ii) Violation of federal and state regulatory limits may occur due to inaccurate data processing and exclusion of branched isomers from analysis.
(iii) Selection and optimization of treatment technologies are contingent on the isomeric distribution of PFASs in source waters;
(iv) Research needs on degradation rates, reaction mechanisms, and competitive sorption of specific isomers in environmentally realistic mixtures; and
(v) Consideration of the behavior and transformation of different isomers of PFAS precursors and their impact on the final results of different water treatment technologies.

■ AUTHOR INFORMATION

Corresponding Author

Arjun K. Venkatesan − *Department of Civil Engineering, Stony Brook University, Stony Brook, New York 11794, United States; New York State Center for Clean Water Technology and School of Marine and Atmospheric Sciences, Stony Brook University, Stony Brook, New York 11794, United States;* orcid.org/0000-0001-9760-9004; Phone: +1 631-632-1998; Email: arjun.venkatesan@stonybrook.edu

Authors

Kaushik Londhe − *Department of Civil Engineering, Stony Brook University, Stony Brook, New York 11794, United States; New York State Center for Clean Water Technology, Stony Brook University, Stony Brook, New York 11794, United States;* orcid.org/0000-0002-0264-6118

Cheng-Shiuan Lee − *New York State Center for Clean Water Technology, Stony Brook University, Stony Brook, New York 11794, United States; Research Center for Environmental Changes, Academia Sinica, Taipei 115, Taiwan;* orcid.org/0000-0001-7582-8193

Carrie A. McDonough − *Department of Civil Engineering, Stony Brook University, Stony Brook, New York 11794, United States; Department of Chemistry, Carnegie Mellon University, Pittsburgh, Pennsylvania 15213, United States;* orcid.org/0000-0001-5152-8495

Complete contact information is available at: https://pubs.acs.org/10.1021/acs.est.2c05518

Notes

The authors declare no competing financial interest.

■ ACKNOWLEDGMENTS

The authors acknowledge the financial support of this work by the Division of Chemical, Bioengineering, Environmental, and Transport Systems (CBET-2052772) of the US National Science Foundation and a grant to the Center for Clean Water Technology (CCWT) from the New York State Department of Health. The content is solely the responsibility of the authors and does not necessarily represent the official views of the sponsors.

■ REFERENCES

(1) Benskin, J. P.; Yeung, L. W. Y.; Yamashita, N.; Taniyasu, S.; Lam, P. K. S.; Martin, J. W. Perfluorinated Acid Isomer Profiling in Water and Quantitative Assessment of Manufacturing Source. *Environ. Sci. Technol.* **2010**, *44*, 9049−9054.

(2) Buck, R. C.; Franklin, J.; Berger, U.; Conder, J. M.; Cousins, I. T.; de Voogt, P.; Jensen, A. A.; Kannan, K.; Mabury, S. A.; van Leeuwen, S. P. Perfluoroalkyl and polyfluoroalkyl substances in the environment: terminology, classification, and origins. *Integr Environ. Assess Manag* **2011**, *7* (4), 513−41.

(3) Benotti, M. J.; Fernandez, L. A.; Peaslee, G. F.; Douglas, G. S.; Uhler, A. D.; Emsbo-Mattingly, S. A forensic approach for distinguishing PFAS materials. *Environmental Forensics* **2020**, *21* (3−4), 319−333.

(4) Reagen, W. K. L. K. R.; Jacoby, C. B.; Purcell, R. G.; Kestner, T. A.; Payfer, R. M.; Miller, J. W. In *Environmental Characterization of 3M Electrochemical Fluorination Derived Perfluorooctanoate and Perfluorooctanesulfonate*, 28th North American meeting, Milwaukee, WI, November; Society of Environmental Toxicology and Chemistry: Milwaukee, WI, 2007.

(5) Benskin, J. P.; De Silva, A. O.; Martin, J. W. Isomer profiling of perfluorinated substances as a tool for source tracking: a review of early findings and future applications. *Rev. Environ. Contam. Toxicol.* **2010**, *208*, 111−160.

(6) De Silva, A. O.; Muir, D. C.G.; Mabury, S. A. Distribution of perfluorocarboxylate isomers in select samples from the North American environment. *Environ. Toxicol. Chem.* **2009**, *28*, 1801−1814.

(7) Schulz, K.; Silva, M. R.; Klaper, R. Distribution and effects of branched versus linear isomers of PFOA, PFOS, and PFHxS: A review of recent literature. *Sci. Total Environ.* **2020**, *733*, 139186.

(8) Wang, Z.; MacLeod, M.; Cousins, I. T.; Scheringer, M.; Hungerbühler, K. Using COSMOtherm to predict physicochemical properties of poly- and perfluorinated alkyl substances (PFASs). *Environmental Chemistry* **2011**, *8* (4), 389.

(9) Rayne, S.; Forest, K. Comparative semiempirical, ab initio, and density functional theory study on the thermodynamic properties of linear and branched perfluoroalkyl sulfonic acids/sulfonyl fluorides, perfluoroalkyl carboxylic acid/acyl fluorides, and perhydroalkyl sulfonic acids, alkanes, and alcohols. *Journal of Molecular Structure: THEOCHEM* **2010**, *941* (1−3), 107−118.

(10) Chen, X.; Zhu, L.; Pan, X.; Fang, S.; Zhang, Y.; Yang, L. Isomeric specific partitioning behaviors of perfluoroalkyl substances in water dissolved phase, suspended particulate matters and sediments in Liao River Basin and Taihu Lake, China. *Water Res.* **2015**, *80*, 235−44.

(11) Chen, M.; Wang, Q.; Shan, G.; Zhu, L.; Yang, L.; Liu, M. Occurrence, partitioning and bioaccumulation of emerging and legacy

per- and polyfluoroalkyl substances in Taihu Lake, China. *Sci. Total Environ.* **2018**, *634*, 251−259.

(12) Yu, N.; Shi, W.; Zhang, B.; Su, G.; Feng, J.; Zhang, X.; Wei, S.; Yu, H. Occurrence of perfluoroalkyl acids including perfluorooctane sulfonate isomers in Huai River Basin and Taihu Lake in Jiangsu Province, China. *Environ. Sci. Technol.* **2013**, *47* (2), 710−7.

(13) Belkouteb, N.; Franke, V.; McCleaf, P.; Kohler, S.; Ahrens, L. Removal of per- and polyfluoroalkyl substances (PFASs) in a full-scale drinking water treatment plant: Long-term performance of granular activated carbon (GAC) and influence of flow-rate. *Water Res.* **2020**, *182*, 115913.

(14) Eschauzier, C.; Beerendonk, E.; Scholte-Veenendaal, P.; De Voogt, P. Impact of treatment processes on the removal of perfluoroalkyl acids from the drinking water production chain. *Environ. Sci. Technol.* **2012**, *46* (3), 1708−15.

(15) McCleaf, P.; Englund, S.; Ostlund, A.; Lindegren, K.; Wiberg, K.; Ahrens, L. Removal efficiency of multiple poly- and perfluoroalkyl substances (PFASs) in drinking water using granular activated carbon (GAC) and anion exchange (AE) column tests. *Water Res.* **2017**, *120*, 77−87.

(16) Gu, Y.; Dong, W.; Luo, C.; Liu, T. Efficient Reductive Decomposition of Perfluorooctanesulfonate in a High Photon Flux UV/Sulfite System. *Environ. Sci. Technol.* **2016**, *50* (19), 10554−10561.

(17) Trojanowicz, M.; Bartosiewicz, I.; Bojanowska-Czajka, A.; Szreder, T.; Bobrowski, K.; Nałecz-Jawecki, G.; Meczyńska-Wielgosz, S.; Nichipor, H. Application of ionizing radiation in decomposition of perfluorooctane sulfonate (PFOS) in aqueous solutions. *Chemical Engineering Journal* **2020**, *379*, 122303.

(18) Park, M.; Daniels, K. D.; Wu, S.; Ziska, A. D.; Snyder, S. A. Magnetic ion-exchange (MIEX) resin for perfluorinated alkylsubstance (PFAS) removal in groundwater: Roles of atomic charges for adsorption. *Water Res.* **2020**, *181*, 115897.

(19) Park, M.; Wu, S.; Lopez, I. J.; Chang, J. Y.; Karanfil, T.; Snyder, S. A. Adsorption of perfluoroalkyl substances (PFAS) in groundwater by granular activated carbons: Roles of hydrophobicity of PFAS and carbon characteristics. *Water Res.* **2020**, *170*, 115364.

(20) Rodowa, A. E.; Knappe, D. R. U.; Chiang, S.-Y. D.; Pohlmann, D.; Varley, C.; Bodour, A.; Field, J. A. Pilot scale removal of per- and polyfluoroalkyl substances and precursors from AFFF-impacted groundwater by granular activated carbon. *Environmental Science: Water Research & Technology* **2020**, *6* (4), 1083−1094.

(21) Ochoa-Herrera, V.; Sierra-Alvarez, R.; Somogyi, A.; Jacobsen, N. E.; Wysocki, V. H.; Field, J. A. Reductive Defluorination of PFOS. *Environ. Sci. Technol. Lett.* **2008**, *42*, 3260−3264.

(22) Charbonnet, J. A.; Rodowa, A. E.; Joseph, N. T.; Guelfo, J. L.; Field, J. A.; Jones, G. D.; Higgins, C. P.; Helbling, D. E.; Houtz, E. F. Environmental Source Tracking of Per- and Polyfluoroalkyl Substances within a Forensic Context: Current and Future Techniques. *Environ. Sci. Technol.* **2021**, *55* (11), 7237−7245.

(23) Gao, Y.; Liang, Y.; Gao, K.; Wang, Y.; Wang, C.; Fu, J.; Wang, Y.; Jiang, G.; Jiang, Y. Levels, spatial distribution and isomer profiles of perfluoroalkyl acids in soil, groundwater and tap water around a manufactory in China. *Chemosphere* **2019**, *227*, 305−314.

(24) McDonough, C. A.; Choyke, S.; Barton, K. E.; Mass, S.; Starling, A. P.; Adgate, J. L.; Higgins, C. P. Unsaturated PFOS and Other PFASs in Human Serum and Drinking Water from an AFFF-Impacted Community. *Environ. Sci. Technol.* **2021**, *55*, 8139.

(25) Liu, J.; Zhong, G.; Li, W.; Mejia Avendaño, S. Isomer-specific biotransformation of perfluoroalkyl sulfonamide compounds in aerobic soil. *Science of The Total Environment* **2019**, *651*, 766−774.

(26) Chen, M.; Qiang, L.; Pan, X.; Fang, S.; Han, Y.; Zhu, L. In Vivo and in Vitro Isomer-Specific Biotransformation of Perfluorooctane Sulfonamide in Common Carp (Cyprinus carpio). *Environ. Sci. Technol.* **2015**, *49* (23), 13817−24.

(27) Benskin, J. P. *Application of Perfluorinated Acid Isomer Profiles for Manufacturing and Exposure Source Determination*, Ph.D. Thesis, University of Alberta, 2011.

(28) Ali, A. M.; Higgins, C. P.; Alarif, W. M.; Al-Lihaibi, S. S.; Ghandourah, M.; Kallenborn, R. Per- and polyfluoroalkyl substances (PFASs) in contaminated coastal marine waters of the Saudi Arabian Red Sea: a baseline study. *Environ. Sci. Pollut Res. Int.* **2021**, *28* (3), 2791−2803.

(29) Ali, A. M.; Langberg, H. A.; Hale, S. E.; Kallenborn, R.; Hartz, W. F.; Mortensen, A. K.; Ciesielski, T. M.; McDonough, C. A.; Jenssen, B. M.; Breedveld, G. D. The fate of poly- and perfluoroalkyl substances in a marine food web influenced by land-based sources in the Norwegian Arctic. *Environ. Sci. Process Impacts* **2021**, *23* (4), 588−604.

(30) Baabish, A.; Sobhanei, S.; Fiedler, H. Priority perfluoroalkyl substances in surface waters - A snapshot survey from 22 developing countries. *Chemosphere* **2021**, *273*, 129612.

(31) Benskin, J. P.; Ahrens, L.; Muir, D. C.; Scott, B. F.; Spencer, C.; Rosenberg, B.; Tomy, G.; Kylin, H.; Lohmann, R.; Martin, J. W. Manufacturing origin of perfluorooctanoate (PFOA) in Atlantic and Canadian Arctic seawater. *Environ. Sci. Technol.* **2012**, *46* (2), 677−85.

(32) Casal, P.; Gonzalez-Gaya, B.; Zhang, Y.; Reardon, A. J.; Martin, J. W.; Jimenez, B.; Dachs, J. Accumulation of Perfluoroalkylated Substances in Oceanic Plankton. *Environ. Sci. Technol.* **2017**, *51* (5), 2766−2775.

(33) Fang, S.; Chen, X.; Zhao, S.; Zhang, Y.; Jiang, W.; Yang, L.; Zhu, L. Trophic magnification and isomer fractionation of perfluoroalkyl substances in the food web of Taihu Lake, China. *Environ. Sci. Technol.* **2014**, *48* (4), 2173−82.

(34) Feng, X.; Ye, M.; Li, Y.; Zhou, J.; Sun, B.; Zhu, Y.; Zhu, L. Potential sources and sediment-pore water partitioning behaviors of emerging per/polyfluoroalkyl substances in the South Yellow Sea. *J. Hazard Mater.* **2020**, *389*, 122124.

(35) Furdui, V. I; Helm, P. A.; Crozier, P. W.; Lucaciu, C.; Reiner, E. J.; Marvin, C. H.; Whittle, D. M.; Mabury, S. A.; Tomy, G. T. Temporal Trends of Perfluoroalkyl Compounds with Isomer Analysis in Lake Trout from Lake Ontario (1979−2004). *Environ. Sci. Technol.* **2008**, *42*, 4739−4744.

(36) Gobelius, L.; Hedlund, J.; Durig, W.; Troger, R.; Lilja, K.; Wiberg, K.; Ahrens, L. Per- and Polyfluoroalkyl Substances in Swedish Groundwater and Surface Water: Implications for Environmental Quality Standards and Drinking Water Guidelines. *Environ. Sci. Technol.* **2018**, *52* (7), 4340−4349.

(37) Houde, M.; Czub, G.; Small, J. M.; Backus, S.; Wang, X.; Alaee, M.; Muir, D. C.G. Fractionation and bioaccumulation of perfluorooctane sulfonate (PFOS) isomers in a Lake Ontario food web. *Environ. Sci. Technol. Lett.* **2008**, *42*, 9397−9403.

(38) Hu, H.; Zhang, Y.; Zhao, N.; Xie, J.; Zhou, Y.; Zhao, M.; Jin, H. Legacy and emerging poly- and perfluorochemicals in seawater and sediment from East China Sea. *Sci. Total Environ.* **2021**, *797*, 149052.

(39) Johansson, J. H.; Salter, M. E.; Acosta Navarro, J. C.; Leck, C.; Nilsson, E. D.; Cousins, I. T. Global transport of perfluoroalkyl acids via sea spray aerosol. *Environ. Sci. Process Impacts* **2019**, *21* (4), 635−649.

(40) Kärrman, A.; Elgh-Dalgren, K.; Lafossas, C.; Møskeland, T. Environmental levels and distribution of structural isomers of perfluoroalkyl acids after aqueous fire-fighting foam (AFFF) contamination. *Environmental Chemistry* **2011**, *8* (4), 372.

(41) Senthil Kumar, K.; Zushi, Y.; Masunaga, S.; Gilligan, M.; Pride, C.; Sajwan, K. S. Perfluorinated organic contaminants in sediment and aquatic wildlife, including sharks, from Georgia, USA. *Mar. Pollut. Bull.* **2009**, *58*, 621−629.

(42) Langberg, H. A.; Arp, H. P. H.; Breedveld, G. D.; Slinde, G. A.; Hoiseter, A.; Gronning, H. M.; Jartun, M.; Rundberget, T.; Jenssen, B. M.; Hale, S. E. Paper product production identified as the main source of per- and polyfluoroalkyl substances (PFAS) in a Norwegian lake: Source and historic emission tracking. *Environ. Pollut.* **2021**, *273*, 116259.

(43) Lutz Ahrens, L. V., Karin, W. *Analysis of Per- and Polyfluoroalkyl Substances (PFASs) and Phenolic Compounds in Swedish Rivers over*

Four Different Seasons; Swedish University of Agricultural Sciences: Uppsala, 2018.
(44) Ma, X.; Shan, G.; Chen, M.; Zhao, J.; Zhu, L. Riverine inputs and source tracing of perfluoroalkyl substances (PFASs) in Taihu Lake, China. *Sci. Total Environ.* **2018**, *612*, 18−25.
(45) Munoz, G.; Labadie, P.; Botta, F.; Lestremau, F.; Lopez, B.; Geneste, E.; Pardon, P.; Devier, M. H.; Budzinski, H. Occurrence survey and spatial distribution of perfluoroalkyl and polyfluoroalkyl surfactants in groundwater, surface water, and sediments from tropical environments. *Sci. Total Environ.* **2017**, *607*−*608*, 243−252.
(46) Picard, J.-C.; Munoz, G.; Vo Duy, S.; Sauvé, S. Longitudinal and vertical variations of waterborne emerging contaminants in the St. Lawrence Estuary and Gulf during winter conditions. *Science of The Total Environment* **2021**, *777*, 146073.
(47) Powley, C. R.; George, S. W.; Russell, M. H.; Hoke, R. A.; Buck, R. C. Polyfluorinated chemicals in a spatially and temporally integrated food web in the Western Arctic. *Chemosphere* **2008**, *70* (4), 664−72.
(48) Roscales, J. L.; Suarez de Puga, B. R.; Vicente, A.; Munoz-Arnanz, J.; Sanchez, A. I.; Ros, M.; Jimenez, B. Levels and trends of perfluoroalkyl acids (PFAAs) in water (2013−2020) and fish from selected riverine basins in Spain. *Chemosphere* **2022**, *286*, 131940.
(49) Shan, G.; Qian, X.; Chen, X.; Feng, X.; Cai, M.; Yang, L.; Chen, M.; Zhu, L.; Zhang, S. Legacy and emerging per- and poly-fluoroalkyl substances in surface seawater from northwestern Pacific to Southern Ocean: Evidences of current and historical release. *J. Hazard Mater.* **2021**, *411*, 125049.
(50) Shi, Y.; Vestergren, R.; Nost, T. H.; Zhou, Z.; Cai, Y. Probing the Differential Tissue Distribution and Bioaccumulation Behavior of Per- and Polyfluoroalkyl Substances of Varying Chain-Lengths, Isomeric Structures and Functional Groups in Crucian Carp. *Environ. Sci. Technol.* **2018**, *52* (8), 4592−4600.
(51) Zhou, J.; Li, S.; Liang, X.; Feng, X.; Wang, T.; Li, Z.; Zhu, L. First report on the sources, vertical distribution and human health risks of legacy and novel per- and polyfluoroalkyl substances in groundwater from the Loess Plateau, China. *J. Hazard Mater.* **2021**, *404* (Pt A), 124134.
(52) Jiang, W.; Zhang, Y.; Zhu, L.; Deng, J. Serum levels of perfluoroalkyl acids (PFAAs) with isomer analysis and their associations with medical parameters in Chinese pregnant women. *Environ. Int.* **2014**, *64*, 40−7.
(53) Torres, F. J.; Ochoa-Herrera, V.; Blowers, P.; Sierra-Alvarez, R. Ab initio study of the structural, electronic, and thermodynamic properties of linear perfluorooctane sulfonate (PFOS) and its branched isomers. *Chemosphere* **2009**, *76* (8), 1143−9.
(54) Xu, Y.; Fletcher, T.; Pineda, D.; Lindh, C. H.; Nilsson, C.; Glynn, A.; Vogs, C.; Norstrom, K.; Lilja, K.; Jakobsson, K.; Li, Y. Serum Half-Lives for Short- and Long-Chain Perfluoroalkyl Acids after Ceasing Exposure from Drinking Water Contaminated by Firefighting Foam. *Environ. Health Perspect.* **2020**, *128* (7), 077004.
(55) McDonough, C. A.; Choyke, S.; Ferguson, P. L.; DeWitt, J. C.; Higgins, C. P. Bioaccumulation of Novel Per- and Polyfluoroalkyl Substances in Mice Dosed with an Aqueous Film-Forming Foam. *Environ. Sci. Technol.* **2020**, *54*, 5700−5709.
(56) De Silva, A. O.; Benskin, J. P.; Martin, L. J.; Arsenault, G.; McCrindle, R.; Riddell, N.; Martin, J. W.; Mabury, S. A. Disposition of perfluorinated acid isomers in sprague-dawley rats; Part 2: Subchronic dose. *Environ. Toxicol. Chem.* **2009**, *28*, 555−567.
(57) Beesoon, S.; Martin, J. W. Isomer-Specific Binding Affinity of Perfluorooctanesulfonate (PFOS) and Perfluorooctanoate (PFOA) to Serum Proteins. *Environ. Sci. Technol.* **2015**, *49* (9), 5722−31.
(58) Yu, N.; Wang, X.; Zhang, B.; Yang, J.; Li, M.; Li, J.; Shi, W.; Wei, S.; Yu, H. Distribution of perfluorooctane sulfonate isomers and predicted risk of thyroid hormonal perturbation in drinking water. *Water Res.* **2015**, *76*, 171−80.
(59) Ng, C. A.; Hungerbuhler, K. Bioaccumulation of perfluorinated alkyl acids: observations and models. *Environ. Sci. Technol.* **2014**, *48* (9), 4637−48.
(60) Armitage, J. M.; Erickson, R. J.; Luckenbach, T.; Ng, C. A.; Prosser, R. S.; Arnot, J. A.; Schirmer, K.; Nichols, J. W. Assessing the bioaccumulation potential of ionizable organic compounds: Current knowledge and research priorities. *Environ. Toxicol. Chem.* **2017**, *36* (4), 882−897.
(61) Han, X.; Nabb, D. L.; Russell, M. H.; Kennedy, G. L.; Rickard, R. W. Renal elimination of perfluorocarboxylates (PFCAs). *Chem. Res. Toxicol.* **2012**, *25* (1), 35−46.
(62) Weaver, Y. M.; Ehresman, D. J.; Butenhoff, J. L.; Hagenbuch, B. Roles of rat renal organic anion transporters in transporting perfluorinated carboxylates with different chain lengths. *Toxicol. Sci.* **2010**, *113* (2), 305−14.
(63) Ross, M. S.; Wong, C. S.; Martin, J. W. Isomer-specific biotransformation of perfluorooctane sulfonamide in Sprague-Dawley rats. *Environ. Sci. Technol.* **2012**, *46* (6), 3196−203.
(64) McDonough, C. A.; Li, W.; Bischel, H. N.; De Silva, A. O.; DeWitt, J. C. Widening the Lens on PFASs: Direct Human Exposure to Perfluoroalkyl Acid Precursors (pre-PFAAs). *Environ. Sci. Technol.* **2022**, *56*, 6004.
(65) Schultes, L.; Vestergren, R.; Volkova, K.; Westberg, E.; Jacobson, T.; Benskin, J. P. Per- and polyfluoroalkyl substances and fluorine mass balance in cosmetic products from the Swedish market: implications for environmental emissions and human exposure. *Environ. Sci. Process Impacts* **2018**, *20* (12), 1680−1690.
(66) Rodgers, K. M.; Swartz, C. H.; Occhialini, J.; Bassignani, P.; McCurdy, M.; Schaider, L. A. How Well Do Product Labels Indicate the Presence of PFAS in Consumer Items Used by Children and Adolescents? *Environ. Sci. Technol.* **2022**, *56* (10), 6294−6304.
(67) Liu, J.; Van Hoomissen, D. J.; Liu, T.; Maizel, A.; Huo, X.; Fernández, S. R.; Ren, C.; Xiao, X.; Fang, Y.; Schaefer, C. E.; Higgins, C. P.; Vyas, S.; Strathmann, T. J. Reductive Defluorination of Branched Per- and Polyfluoroalkyl Substances with Cobalt Complex Catalysts. *Environmental Science & Technology Letters* **2018**, *5* (5), 289−294.
(68) Uwayezu, J. N.; Yeung, L. W. Y.; Backstrom, M. Sorption of PFOS isomers on goethite as a function of pH, dissolved organic matter (humic and fulvic acid) and sulfate. *Chemosphere* **2019**, *233*, 896−904.
(69) Yamamoto, T.; Noma, Y.; Sakai, S.; Shibata, Y. Photodegradation of perfluorooctane sulfonate by UV irradiation in water and alkaline 2-propanol. *Environ. Sci. Technol.* **2007**, *41* (16), 5660−5.
(70) Tenorio, R.; Liu, J.; Xiao, X.; Maizel, A.; Higgins, C. P.; Schaefer, C. E.; Strathmann, T. J. Destruction of Per- and Polyfluoroalkyl Substances (PFASs) in Aqueous Film-Forming Foam (AFFF) with UV-Sulfite Photoreductive Treatment. *Environ. Sci. Technol.* **2020**, *54* (11), 6957−6967.
(71) Chaplin, B. P. Critical review of electrochemical advanced oxidation processes for water treatment applications. *Environ. Sci. Process Impacts* **2014**, *16* (6), 1182−203.
(72) Radjenovic, J.; Sedlak, D. L. Challenges and Opportunities for Electrochemical Processes as Next-Generation Technologies for the Treatment of Contaminated Water. *Environ. Sci. Technol.* **2015**, *49* (19), 11292−302.
(73) Uwayezu, J. N.; Carabante, I.; Lejon, T.; van Hees, P.; Karlsson, P.; Hollman, P.; Kumpiene, J. Electrochemical degradation of per- and poly-fluoroalkyl substances using boron-doped diamond electrodes. *J. Environ. Manage* **2021**, *290*, 112573.
(74) Wang, Y.; Pierce, R. D.; Shi, H.; Li, C.; Huang, Q. Electrochemical degradation of perfluoroalkyl acids by titanium suboxide anodes. *Environmental Science: Water Research & Technology* **2020**, *6* (1), 144−152.
(75) Vyas, S. M.; Kania-Korwel, I.; Lehmler, H. J. Differences in the isomer composition of perfluoroctanesulfonyl (PFOS) derivatives. *J. Environ. Sci. Health A Tox Hazard Subst Environ. Eng.* **2007**, *42* (3), 249−55.
(76) Benskin, J. P.; Bataineh, M.; Martin, J. W. Simultaneous Characterization of Perfluoroalkyl Carboxylate, Sulfonate, and Sulfonamide Isomers by Liquid Chromatography-Tandem Mass Spectrometry. *Anal. Chem.* **2007**, *79* (17), 6455−6464.

(77) Ahrens, L.; Gashaw, H.; Sjoholm, M.; Gebrehiwot, S. G.; Getahun, A.; Derbe, E.; Bishop, K.; Akerblom, S. Poly- and perfluoroalkylated substances (PFASs) in water, sediment and fish muscle tissue from Lake Tana, Ethiopia and implications for human exposure. *Chemosphere* **2016**, *165*, 352−357.
(78) Trojanowicz, M.; Bartosiewicz, I.; Bojanowska-Czajka, A.; Kulisa, K.; Szreder, T.; Bobrowski, K.; Nichipor, H.; Garcia-Reyes, J. F.; Nałecz-Jawecki, G.; Meczyńska-Wielgosz, S.; Kisała, J. Application of ionizing radiation in decomposition of perfluorooctanoate (PFOA) in waters. *Chem. Eng. J.* **2019**, *357*, 698−714.
(79) Barzen-Hanson, K. A.; Roberts, S. C.; Choyke, S.; Oetjen, K.; McAlees, A.; Riddell, N.; McCrindle, R.; Ferguson, P. L.; Higgins, C. P.; Field, J. A. Discovery of 40 Classes of Per- and Polyfluoroalkyl Substances in Historical Aqueous Film-Forming Foams (AFFFs) and AFFF-Impacted Groundwater. *Environ. Sci. Technol.* **2017**, *51* (4), 2047−2057.
(80) Langlois, I.; Oehme, M. Structural identification of isomers present in technical perfluorooctane sulfonate by tandem mass spectrometry. *Rapid Commun. Mass Spectrom.* **2006**, *20* (5), 844−50.
(81) Martin, J. W.; Kannan, K.; Berger, U.; Voogt, P. D.; Field, J.; Franklin, J.; Giesy, J. P.; Harner, T.; Muir, D. C. G.; Scott, B.; Kaiser, M.; Jarnberg, U.; Jones, K. C.; Mabury, S. A.; Schroeder, H.; Simcik, M.; Sottani, C.; Bavel, B. V.; Karrman, A.; Lindstrom, G.; Leeuwen, S. V. Analytical challenges hamper perfluoroalkyl research. *Environ. Sci. Technol.* **2004**, *38*, 248A−255A.
(82) Riddell, N.; Arsenault, G.; Benskin, J. P.; Chittim, B.; Martin, J. W.; McAlees, A.; McCrindle, R. Branched Perfluorooctane Sulfonate Isomer Quantification and Characterization in Blood Serum Samples by HPLC/ESI-MS(/MS). *Environ. Sci. Technol.* **2009**, *43*, 7902−7908.
(83) Bagenstose, K. New Jersey approves drinking water standards for toxic PFAS chemicals. Will legal battles follow? *USA Today*, https://www.usatoday.com/story/news/2020/04/07/new-jersey-approves-drinking-water-standards-toxic-pfas-chemicals/2963032001/ (accessed November 2020).
(84) State-by-State Regulation of PFAS Substances in Drinking Water. https://www.bclplaw.com/en-US/insights/state-by-state-regulation-of-pfas-substances-in-drinking-water.html (accessed June 15, 2021).
(85) Per- and Polyfluoroalkyl Substances (PFAS) Summary of State Regulation to Protect Drinking Water. https://www.awwa.org/Portals/0/AWWA/Government/SummaryofStateRegulationtoProtectDrinkingWater.pdf (accessed 06/23/2021).
(86) California Issues the Nation's Strictest Notice Levels for PFAS in Drinking Water. https://www.bbklaw.com/news-events/insights/2019/legal-alerts/09/california-issues-the-nations-strictest-notice-le (accessed November 2020).
(87) Lin, H.; Wang, Y.; Niu, J.; Yue, Z.; Huang, Q. Efficient Sorption and Removal of Perfluoroalkyl Acids (PFAAs) from Aqueous Solution by Metal Hydroxides Generated in Situ by Electrocoagulation. *Environ. Sci. Technol.* **2015**, *49* (17), 10562−9.
(88) Fenti, A.; Jin, Y.; Rhoades, A. J. H.; Dooley, G. P.; Iovino, P.; Salvestrini, S.; Musmarra, D.; Mahendra, S.; Peaslee, G. F.; Blotevogel, J. Performance testing of mesh anodes for in situ electrochemical oxidation of PFAS. *Chemical Engineering Journal Advances* **2022**, *9*, 100205.
(89) Shi, H.; Wang, Y.; Li, C.; Pierce, R.; Gao, S.; Huang, Q. Degradation of Perfluorooctanesulfonate by Reactive Electrochemical Membrane Composed of Magneli Phase Titanium Suboxide. *Environ. Sci. Technol.* **2019**, *53*, 14528.
(90) Kim, T. H.; Yu, S.; Choi, Y.; Jeong, T. Y.; Kim, S. D. Profiling the decomposition products of perfluorooctane sulfonate (PFOS) irradiated using an electron beam. *Sci. Total Environ.* **2018**, *631−632*, 1295−1303.
(91) Londhe, K.; Lee, C.-S.; Zhang, Y.; Grdanovska, S.; Kroc, T.; Cooper, C. A.; Venkatesan, A. K. Energy Evaluation of Electron Beam Treatment of Perfluoroalkyl Substances in Water: A Critical Review. *ACS ES&T Engineering* **2021**, *1*, 827.
(92) Patch, D.; O'Connor, N.; Koch, I.; Cresswell, T.; Hughes, C.; Davies, J. B.; Scott, J.; O'Carroll, D.; Weber, K. Elucidating degradation mechanisms for a range of per- and polyfluoroalkyl substances (PFAS) via controlled irradiation studies. *Sci. Total Environ.* **2022**, *832*, 154941.
(93) Park, S.; de Perre, C.; Lee, L. S. Alternate Reductants with VB12 to Transform C8 and C6 Perfluoroalkyl Sulfonates: Limitations and Insights into Isomer-Specific Transformation Rates, Products and Pathways. *Environ. Sci. Technol.* **2017**, *51* (23), 13869−13877.
(94) Wang, S.; Yang, Q.; Chen, F.; Sun, J.; Luo, K.; Yao, F.; Wang, X.; Wang, D.; Li, X.; Zeng, G. Photocatalytic degradation of perfluorooctanoic acid and perfluorooctane sulfonate in water: A critical review. *Chemical Engineering Journal* **2017**, *328*, 927−942.
(95) Jin, L.; Zhang, P. Photochemical decomposition of perfluorooctane sulfonate (PFOS) in an anoxic alkaline solution by 185nm vacuum ultraviolet. *J. Chem. Eng.* **2015**, *280*, 241−247.
(96) Crone, B. C.; Speth, T. F.; Wahman, D. G.; Smith, S. J.; Abulikemu, G.; Kleiner, E. J.; Pressman, J. G. Occurrence of Per- and Polyfluoroalkyl Substances (PFAS) in Source Water and Their Treatment in Drinking Water. *Crit Rev. Environ. Sci. Technol.* **2019**, *49* (24), 2359−2396.
(97) Rahman, M. F.; Peldszus, S.; Anderson, W. B. Behaviour and fate of perfluoroalkyl and polyfluoroalkyl substances (PFASs) in drinking water treatment: a review. *Water Res.* **2014**, *50*, 318−40.
(98) Xiao, F.; Simcik, M. F.; Gulliver, J. S. Mechanisms for removal of perfluorooctane sulfonate (PFOS) and perfluorooctanoate (PFOA) from drinking water by conventional and enhanced coagulation. *Water Res.* **2013**, *47* (1), 49−56.
(99) EPA Announces New Drinking Water Health Advisories for PFAS Chemicals, $1 Billion in Bipartisan Infrastructure Law Funding to Strengthen Health Protections. U.S. EPA, 2022, (accessed June 2022). https://www.epa.gov/newsreleases/epa-announces-new-drinking-water-health-advisories-pfas-chemicals-1-billion-bipartisan.